INITIAL ASSESSMENT OF A SIMPLE FUNCTIONAL IMAGE OF VENTILATION

Nathaniel M. Alpert, Kenneth A. McKusick, John A. Correia, William Shea, Gordon L. Brownell, and Majic S. Potsaid

Massachusetts General Hospital, Boston, Massachusetts

Several methods for quantitatively measuring regional ventilation using an inert gas such as ^{133}Xe have been described. One such method provides a functional image of washout. A particularly simple functional image may be derived from the mean transit time for clearance. Regional ventilation may thus be represented as a single image in which the spatial distribution of washout from multiple small regions of the lung is displayed. In 100 patients for whom such a functional image of ventilation was obtained, the functional image was found to be generally more useful and easier to interpret than sequential images taken during the period of washout. Distributions of half-time ($t_{1/2}$) for washout and the mean transit time ($\bar{t}$) in the same population were similar in shape, but the $\bar{t}$ distribution peaked about 15 sec later than the $t_{1/2}$ distribution. The mathematical simplicity of the functional image described here should permit its implementation on virtually any nuclear medicine computer system.

Because the perfusion lung scan continues to be one of the most difficult studies to interpret in nuclear medicine, many clinics obtain a xenon ventilation study in addition to a careful history and current chest radiograph. The finding of a segmental pulmonary perfusion defect in a patient who has a normal chest radiograph and xenon ventilation study supports a clinical diagnosis of pulmonary embolism. The interpretation of the xenon study depends on the spatial distribution of the xenon at equilibration as well as an assessment of the rate of xenon washout from the lung following equilibration. The rate of washout may be qualitatively assessed from sequential images taken at intervals during washout or quantitatively by measuring the disappearance of radioactivity from several regions of the lung during washout. Precise localization of ventilation defects requires that the clearance rate be computed for many small contiguous regions of the lung, and thus the presentation and interpretation of the clearance rates can become awkward as the amount of data increases. A functional image (*1*) of the clearance rate (often referred to as the washout) provides a single image from which both the regional distribution and magnitude of clearance rate may be observed (*2–6*).

The purpose of this paper is to describe the use of a functional image of clearance rate which we have found to be useful in clinical practice.

METHODS

Xenon-133 was administered by inhalation from a closed spirometer (Warren Collins Corp., Braintree, Mass.) at a concentration of 3 mCi per liter of air. The patient was imaged supine in a posterior projection using a Searle Radiographics Pho/Gamma III HP scintillation camera equipped with a diverging collimator. The patient rebreathed the xenon gas until a constant lung concentration had been achieved; then a 200,000-count equilibrium image was obtained followed by a 2.5-min washout image. These images were acquired on a 64 × 64 matrix under computer control and stored on a magnetic disk for subsequent computer analysis (*6*). In addition, sequential images were made during the washout phase on 35-mm high-contrast copy film at a rate of one every 5 sec.

The data processing steps used to construct the functional image are shown in Table 1. The purpose of the data manipulation was to compute the ratio of the equilibrium count rate to the sum of the counts obtained during washout. This ratio was formed for every picture element (i.e., for every "pixel"). The

Received June 11, 1975; revision accepted Aug. 18, 1975.

For reprints contact: N. M. Alpert, Physics Research Laboratory, Massachusetts General Hospital, 32 Fruit St., Boston, Mass. 02114.

TABLE 1. DATA MANIPULATION

1. Smooth equilibrium image
2. Smooth washout image
3. Zero all pixels in (1) with counts less than 25% maximum pixel
4. Multiply each pixel in (3) by the ratio 60/(frame time in seconds)
5. Compute ratio of (4) to (2) for every pixel
6. Display the resulting ratio image using a linear mapping:

$$\text{Output brightness} = \frac{\text{(max gray level)}}{\text{(max pixel)}} \times \text{(input pixel)}$$

rationale for this procedure is discussed below. Image smoothing was used to reduce statistical fluctuations. The choice of smoothing algorithm is not critical; in our study, a nine-point routine with weights ½ : 1 : ½ was applied twice to each image. Counts recorded outside the lung region, even though they are relatively low, can lead to large but spurious ratio values. Accordingly, all pixels whose values were less than 25% of the maximum pixel in the equilibrium image were arbitrarily set to zero.

Each element in the matrix of values computed by the procedure described in Table 1 represents an estimate of the clearance rate, which is the reciprocal of the mean transit time. The brightness of each pixel in the functional image was made proportional to the magnitude of the clearance rate. Quantitative data were extracted from the functional image by intensifying selected ranges of clearance rates. These ranges were fixed percentages of the maximum clearance rate: 80–100%, 60–80%, and 40–60%. These data may be presented either as percent clearance per minute or as the reciprocal, the mean transit time.

RESULTS

One hundred patients referred for pulmonary embolism studies were examined with a ^{133}Xe ventilation measurement, a standard four-view perfusion lung scan (^{99m}Tc-HAM), and chest x-rays. In each case, a functional image was constructed as described above. These data were correlated with the findings on the chest x-rays, the perfusion lung scan, and with the sequential 5-sec images obtained on 35-mm film during the washout phase.

Several examples, typical of the results obtained by this technique, are presented below. The equilibration distribution of ventilated volume (labeled A) and a posterior view from the perfusion lung scan (B) are shown along with the functional image of clearance rates (C). In some cases quantitative information is provided by superimposing a "Z-cut" on the functional image. Each Z-cut image was derived from the functional image by intensifying a preselected range of clearance rates. Each range is defined as a fraction of the maximum clearance rate [80–100% (D), 60–80% (E), and 40–60% (F)]. For example, a maximum clearance rate of 3.0/min would yield ranges of 91–95, 83–91, and 70–83%/min or, equivalently, in terms of transit times, ranges of 20–25, 25–33, and 33–50 sec.

Normal ventilation and perfusion. Figure 1 shows part of a ventilation–perfusion study in a 51-year-old woman. She presented with pleuritic chest pain of 7 days' duration. The pain started after the patient had been stretching to put up curtains.

The perfusion lung scan was normal, with no evidence of pulmonary embolism.

Ventilation as determined by the xenon equilibrium image and the functional image was also normal, showing no parenchymal disease. The three Z-cuts show that $\bar{t}$ was symmetrically distributed in a pattern similar to that seen in the corresponding perfusion lung scan.

Pulmonary embolism. Figure 2 presents part of a ventilation–perfusion study performed on a 20-year-old man who had suffered a transection of the cervical spinal cord following a motorcycle accident. The patient was quadriplegic. He was referred for a study for possible pulmonary emboli.

The perfusion lung scan showed segmental de-

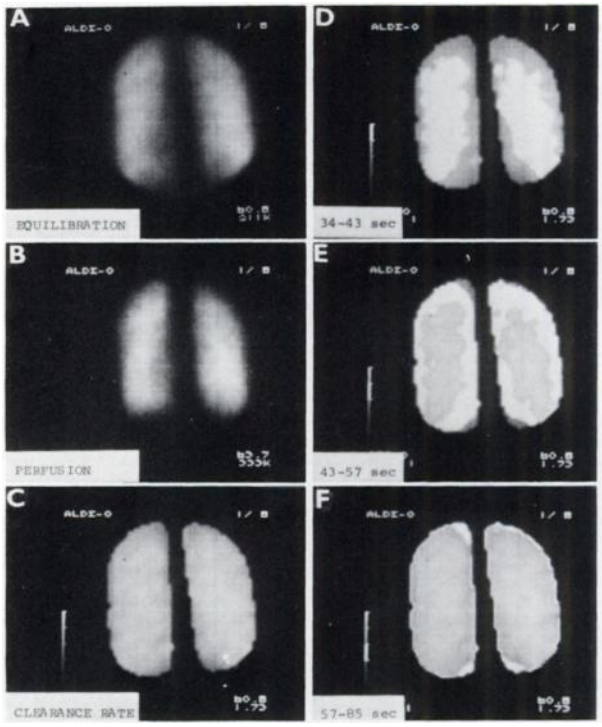

FIG. 1. Normal ventilation–perfusion study. (A) Regional distribution of ventilation at equilibration (^{133}Xe, posterior view); (B) perfusion lung scan (^{99m}Tc-HAM, posterior view); (C) functional image of clearance rate ($1/\bar{t}$); (D) Z-cut: $\bar{t}$ between 34 and 43 sec; (E) Z-cut: $\bar{t}$ between 43 and 57 sec; and (F) Z-cut: $\bar{t}$ between 57 and 85 sec.

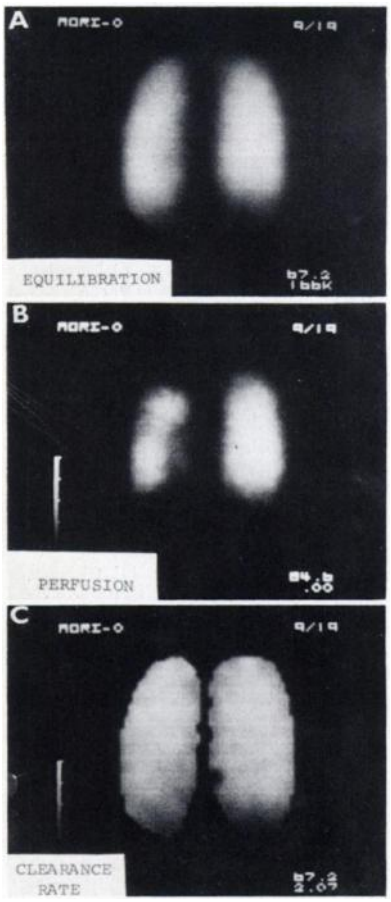

FIG. 2. Pulmonary embolism. (A) Regional distribution of ventilation at equilibration (^{133}Xe, posterior view); (B) perfusion lung scan (^{99m}Tc-HAM, posterior view); and (C) functional image of clearance rate ($1/\bar{t}$).

fects in the left superior and left apical posterior segments.

The spatial distribution of ^{133}Xe at equilibration (A) and the functional image (C) were both normal.

Chronic obstructive pulmonary disease. Figure 3 again shows pertinent parts of a ventilation–perfusion scan done on a 49-year-old woman with known hypothyroidism, chronic bronchitis, and normal chest radiographs. She was referred for lung study because of increasing nonpainful dyspnea. Pulmonary function studies performed after the lung scan showed a "moderate obstructive defect" (1-sec forced expiratory volume vital capacity, 61% of predicted).

The lung scan showed multiple nonsegmental perfusion defects corresponding to the abnormalities seen on both the spatial and functional ventilation images.

Inactive tuberculosis. Figure 4 shows the ventilation–perfusion study obtained on a 42-year-old man with known inactive tuberculosis and (by chest radiography) a right apical granuloma. He was referred for a lung scan because of thrombophlebitis of the right deep saphenous vein.

The lung scan showed nonsegmental perfusion defects of the right lung, corresponding to the abnormal ventilation best seen on the functional image of clearance rates.

DISCUSSION

A xenon ventilation study often consists of three measurements: (A) the regional distribution of the initial breath as an index of ventilation; (B) the regional distribution of xenon at equilibration as an index of ventilated volume; and (C) the regional distribution of xenon clearance from the lung as a more accurate index of ventilation than provided by the initial breath. First-breath maneuvers are difficult to standardize and require patient cooperation. Therefore, most quantitative information in clinical practice has been obtained from the equilibration and washout data. Data obtained during the washout phase of measurement (C) may be analyzed either qualitatively or quantitatively by assessment of sequential images.

Figure 5A is an idealized graph of counts as a function of time for the protocol described above. Many analyses have been applied to such data, most often single-compartment models of washout. We have chosen an analysis which makes no assump-

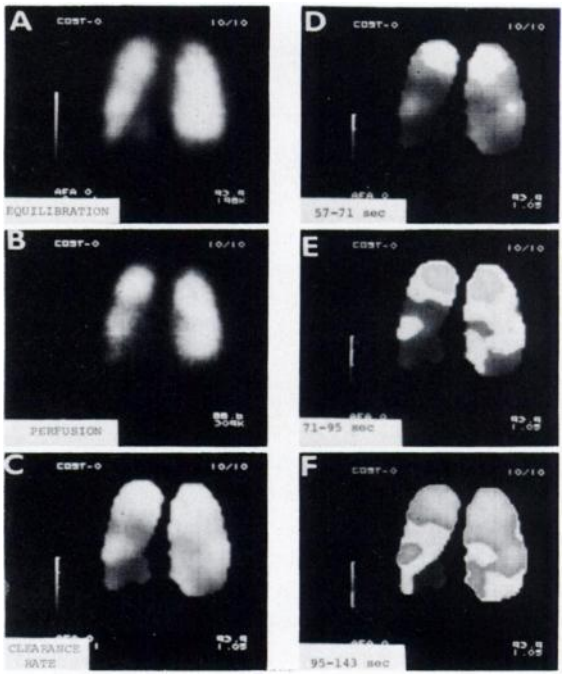

FIG. 3. Chronic obstructive pulmonary disease. (A) Regional distribution of ventilation at equilibration (^{133}Xe, posterior view); (B) perfusion lung scan (^{99m}Tc-HAM, posterior view); (C) functional image of clearance rate ($1/\bar{t}$); (D) Z-cut: $\bar{t}$ between 57 and 71 sec; (E) Z-cut: $\bar{t}$ between 71 and 95 sec; and (F) Z-cut: $\bar{t}$ between 95 and 143 sec.

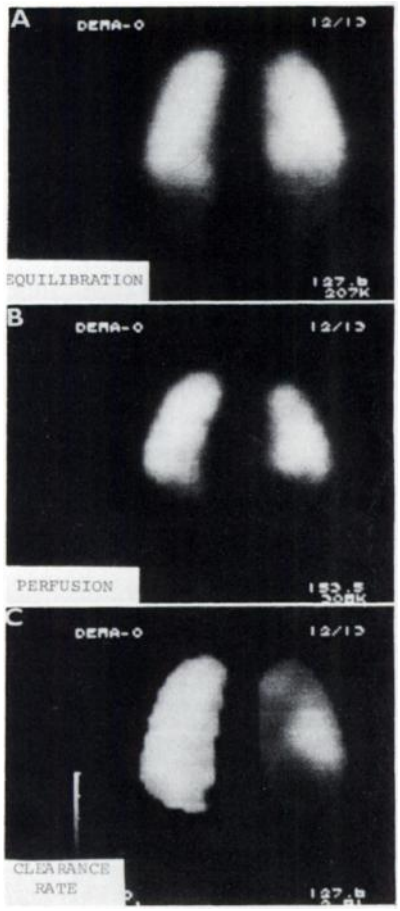

FIG. 4. Inactive tuberculosis. (A) Regional distribution of ventilation at equilibration (^{133}Xe, posterior view); (B) perfusion lung scan (^{99m}Tc-HAM, posterior view); and (C) functional mage of clearance rate ($1/\bar{t}$).

tions regarding either the number of compartments or their interconnections, but which yields a single parameter—the mean transit time. The use of the mean transit time has been validated for regional lung ventilation by Secker-Walker (*7*). The theory of the mean transit time has been described by Zierler (*8*) and will not be repeated here. Instead, we give a plausibility argument in the hope that it will provide more insight than a mathematical derivation.

Figure 5B shows two idealized washout curves. Clearly more counts will be recorded during washout if ventilation is substandard. This inverse relationship between the mean washout time and the number of counts measured during washout is the basis of the technique. The ratio $(\Sigma_i N_i) \div$ (equilibration count rate) yields the mean transit time.

The denominator may be viewed as a scale factor which normalizes the $\Sigma_i N_i$ to the total lung volume viewed by the detector. Note (*8*) that

$$\frac{\Sigma_i N_i}{\text{equilibrium count rate}} = \bar{t} = V/F,$$

where $\bar{t}$ is the mean transit time, V is the volume of distribution, F is the air flow (assumed constant), N is the number of counts within a picture element, and $\Sigma_i N_i$ is the total counts collected during washout.

Figure 6 shows histograms of the conventional half-time index $t_{1/2}$ of washout (*9*) and of the mean transit time $\bar{t}$ obtained from the first 60 patients studied. The shapes of the histograms are similar, but the histogram of $\bar{t}$ values is displaced so that its centroid occurs about 15 sec later than the centroid of the $t_{1/2}$ histogram. That $t_{1/2}$ is typically less than $\bar{t}$ is not surprising since $t_{1/2}$ is computed on the basis of a single-exponential model whereas $\bar{t}$ uses all the data obtained during washout. The data shown in Fig. 6 support the contention of Secker-Walker (*7*) that $\bar{t}$ is an adequate measure of ventilation.

The above protocol allows for a 2.5-min washout measurement. Precise estimation of the mean transit time requires measurement until the count rate falls to zero. This may be impractical in patients with greatly prolonged washout times. In such cases $\bar{t}$ is underestimated, but in clinical use this source of error has not been a problem, since the clearance rate is still markedly decreased.

In the construction of functional images it is more satisfying to display $K = 1/\bar{t}$ instead of the mean transit time. The intensity of the image of K is increased where ventilation is more rapid and conversely decreased in poorly ventilated regions. This conforms to the conventional display of perfusion lung scans where poorly perfused regions are least intense.

CONCLUSION

The functional image of $K = 1/\bar{t}$ provides a clinically useful and quantitative method for assessing regional ventilation in patients being evaluated for

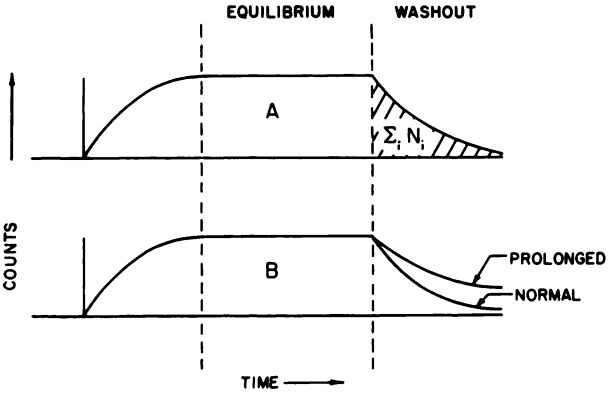

FIG. 5. Idealized representation of curves obtained during regional ventilatory examination with ^{133}Xe. (A) Shading shows area under washout curve. (B) As xenon clearance is prolonged, area under washout curve is increased.

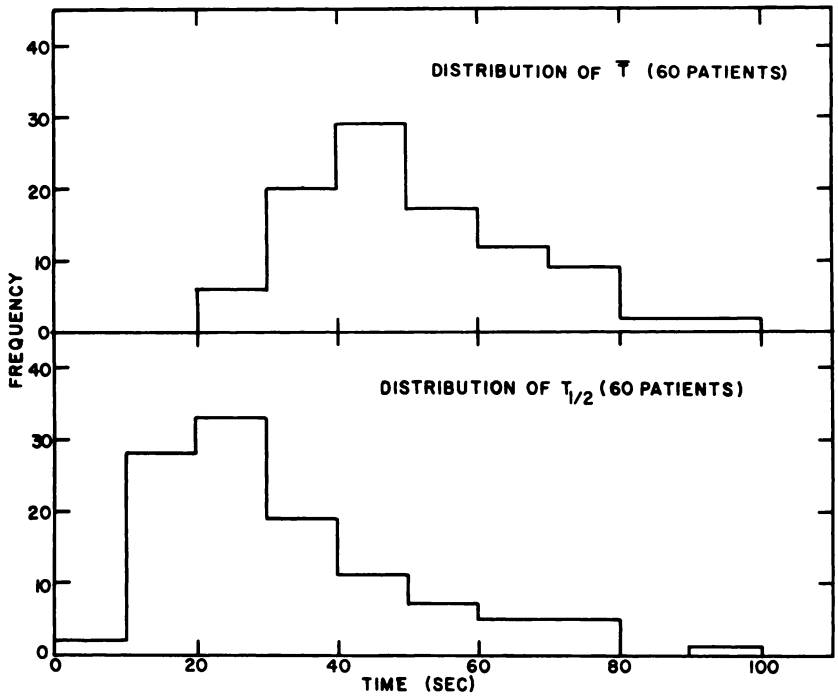

FIG. 6. Distribution of $\bar{t}$ and $t_{1/2}$ in 60 patients referred for evaluation for possible pulmonary embolism.

pulmonary embolism. It is convenient to use and may be easily implemented on any nuclear medicine computer system. The required computations can be done faster than those of any previously described technique (about 10 sec in PDP-9 assembly language). Since both the equilibration and washout images, which form the basis for the functional image, can be measured with good statistical accuracy, a high-quality functional image can be constructed. Our impression is that this easily derived functional image of ventilation often provides information not apparent on standard sequential images taken during washout.

ACKNOWLEDGMENT

This work was supported in part by NIH Grants GM-16712, GM-889, and AEC Contract E(11-1)3333.

REFERENCES

1. ALPERT NM, HOOP B, CHESLER DA, et al: Dynamic studies with a multiprogrammed computer system. In *Dynamic Studies with Radioisotopes in Medicine*, Vienna, IAEA, 1974, pp 27–44

2. MACINTYRE WJ, INKLEY SR: Functional lung scanning with ^{133}Xe. *J Nucl Med* 10: 355, 1969

3. MACINTYRE WJ, DRESCHER WP, INKLEY SR: The future of functional scanning and its dependence on computer-assisted analysis. In *Quantitative Organ Visualization in Nuclear Medicine*, Kenny PJ, Smith EM, eds, Coral Gables, University of Miami Press, 1971, pp 865–890

4. BURDINE JA, ALAGARSAMY V, RYDER LA, et al: Quantitative functional images of regional ventilation and perfusion. *J Nucl Med* 13: 417, 1973

5. WAGNER HN, NATARAJAN TK: Functional imaging. In *Fourth Symposium on Sharing of Computer Programs and Technology in Nuclear Medicine*, McClain WJ, Mashewitz BF, eds, Oak Ridge, Tenn., AEC CONF-740531, 1974, pp 81–88

6. ALPERT NM, BURNHAM CA, DEVEAU LA, et al: NUMEDICS: A system for on-line data processing in nuclear medicine. *J Nucl Med* 16: 386–392, 1975

7. SECKER-WALKER RH, HILL RI, MARKHAM J, et al: The measurement of regional ventilation in man: A new method of quantitation. *J Nucl Med* 14: 725–732, 1973

8. ZIERLER KL: Equations for measuring blood flow by external monitoring of radioisotopes. *Circ Res* 16: 309–321, 1965

9. BENTIVOGLIO LG, BEEREL F, STEWART PB, et al: Studies of regional ventilation and perfusion in pulmonary emphysema using xenon. *Am Rev Respir Dis* 88: 315–329, 1963